Triiodothyronine Regulates the Number and Morphological Development of Supporting Cells of organ of Corti During Critical Periods of Cochlear Development

Xue Bai
Huazhong University of Science and Technology
Kai Xu
Huazhong University of Science and Technology
Sen Chen
Huazhong University of Science and Technology
Le Xie
Huazhong University of Science and Technology
Yue Qiu
Huazhong University of Science and Technology
Yu Sun (sunyu@hust.edu.cn)
Union Hospital of Tongji Medical College of Huazhong University of Science and Technology
https://orcid.org/0000-0002-1771-3715

Research Article

Keywords: Triiodothyronine, Hearing loss, Cochlear remodeling, Organ of Corti

Posted Date: February 7th, 2022

DOI: https://doi.org/10.21203/rs.3.rs-1305245/v1

Abstract

Thyroid hormones are essential for cochlear development and normal auditory function. In rodents, previous study reports that excessive triiodothyronine (T3) accelerates development of cochlear morphology and cause deafness. However, the mechanism of T3 induced hearing loss and its effect on the remodeling of the organ of Corti (OC) remain unclear. In this study, neonatal mice were given T3 at different time points, and then auditory brainstem responses (ABR) and morphological changes of the OC were analyzed at postnatal day (P) 18. Mice treated with T3 at P0 or P1 showed severe hearing loss with disordered stereocilia of the outer hair cells (OHCs), and impaired function of mechanoelectrical transduction of OHCs. In addition, we found that treatment with T3 at P0 or P1 resulted in overproduction of Deiter-like cells (Deiter's cell, DC, a supporting cell in OC). These extra cells have phalangeal process structure similar to DC, and coupled with normal DC by gap junctions. Compared with the control group, the transcription levels of Sox2 and notch pathway related genes in the cochlea of T3 group were significantly down-regulated. Furthermore, T3 treatment combined with downregulation of Sox2 not only resulted in overproduction of DCs, but also led to a large number of ectopic outer Pillar cells (OPCs). This can induce a great change of morphology of OC, forming double tunnels of Corti structure. Together, our study provides new evidence for dual roles of T3 in regulating both hair cell and supporting cell development, suggesting that it is possible to increase the reserve of supporting cells.

Introduction

Organ of Corti (OC), the auditory sensor by which sounds are converted into nerve impulses, is one of the most complex organ structures in human body. The structure includes one row of inner hair cell (IHC) and three rows of outer hair cell (OHC) interdigitated different types of the supporting cell (SC). The morphology of different SCs is distinct and few studies have focus on the biology and function of them[1]. Abnormal development of SCs induced by gene mutations, congenital cytomegalovirus infection or thyroid disease can lead to severe hearing loss[2–4]. Besides, growing evidence suggests that well-formed SCs cells acts as mediators of hair cell development, function and survival. Therefore, further research on the proliferation, maturation and development of SCs may increase our understanding of inner ear development and regeneration.

In rodents, the overall structure of the auditory epithelium is formed by the time of birth and continues to mature structurally until hearing begins at postnatal day (P)14. During this period, HCs form a V-shape stereocilia that accommodates the mechanoelectrical transduction (MET) channels. Deiters' cell, a type of SCs coupled with OHC, extend a phalangeal process to provide structural support for OHC. Inner and outer Pillar cells (PC) form triangular tunnel of Corti (TC) which support the whole OC. More different types of SCs, such as Hensen's cells, Claudious cells or inner sulcus cells, lie lateral to OHC or IHC. A large number of studies have attempted to explore the molecules that manage the proliferation and differentiation of HCs, in the hope of regenerating HCs to achieve the effect of restoring impaired hearing. Above studies focus on multiple regulatory genes (e.g. Atoh1, Gfi1, Pou4f3, Sox2) and signaling pathways (e.g. Wnt, Notch) expressed or activated in cochlear epithelium[5, 6, 1]. Although ectopic hair

cells can be induced in the cochlea of newborn or adult mice, due to the lack of corresponding SCs and fine OC structure, the above-mentioned efforts cannot restore hearing. For the treatment of deafness, reconstruction of the entire OC may be a better but more difficult choice. It is particularly important to explore the development and regeneration of SCs. Interestingly, SCs development is regulated by both local molecular pathways and systemic hormones.

Thyroid hormone (TH) regulates cochlear development and the formation of normal hearing [7, 8]. Triiodothyronine (T3) is the main active form of thyroid hormone and acts on thyroid hormone receptors (TRs) to induce a series of physiological changes in target tissues[9, 10]. In humans, thyroid related-diseases such as endemic iodine deficiency, congenital hypothyroidism, and resistance to T3 caused by mutations in TRs are associated with hearing loss[11–13]. However, the mechanism of hearing loss caused by thyroid disease is still poorly understood. Animals with developmental hypothyroidism exhibit distortion of the tectorial membrane and delayed opening of the tunnel of Corti, which might be the main causes of deafness[14–16]. In addition, secondary hypothyroidism caused by mutations in TRs results in permanent potassium channel dysfunction and impaired HC function[17–19]. Conversely, excessive T3 during critical stages of cochlear development also leads to SC's death in the greater epithelial ridge (GER) and the tunnel of Corti opening in advance with premature PCs[20]. In model species or humans, development of the auditory system is sensitive to T3 signaling, and either systemic hypothyroidism or hyperthyroidism will lead to irreversible hearing loss. The mechanism of thyroid hormone regulation of cochlear development needs to be further studied.

In order to explore T3 effect on remodeling of the organ of Corti and SC's development during early development, we administered T3 to neonatal mice at different time points after birth. Our results show that ectopic T3 given at an early stage (P0 or P1) leads to severe hearing loss with abnormal stereocilia alignment and HC mechanosensory dysfunction. Moreover, treatment with T3 at P0 or P1 resulted in overproduction of Deiter-like cells and these extra cells normally expressed functional markers Connexin30 (Cx30) and acetylated α-tubulin. A series of genes related to the development of cochlear sensory epithelium were significantly down-regulated in the T3 group. When T3 treatment was combined with downregulation of cochlear Sox2 expression, the number of DCs and outer pillar cells (OPCs) increased significantly, and it can induce cochlear epithelium to form an OC with a double TC structure. Our results provide new evidence for the role of T3 in regulating the development of cochlear sensory epithelium in the neonatal mice.

Materials And Methods

Mouse models

Neonatal mouse pups were injected with 2.0 μg of T3 (T2877, Merck KGaA, Darmstadt, Germany) in a volume of 10 μL, or the equivalent volume of saline, at P0 (P0 group), P1 (P1 group) or P3 (P3 group). To study the Notch signaling pathway, DAPT (HY-13027, MCE, Monmouth Junction, NJ, USA) was injected subcutaneously at P0 (250 nmol/g), and then once per day for four consecutive days. Details of the

genotyping process are given in the study by Zhang et al[21]. The genotyping primers used were as follows:

wild type (F) 5'-CTAGGCCACAGAATTGAAAGATCT-3';

wild type (R) 5'-GTAGGTGGAAATTCTAGCATCATCC-3';

mutant (F) 5'-GCG GTCTGGCAGTAAAAACTATC-3';

mutant (R) 5'-GTGAAACAGCAT TGCTGTCACTT-3'.

We performed all animal procedures according to protocols of the Committee on Animal Research of Tongji Medical College, Huazhong University of Science and Technology.

Auditory brainstem response (ABR)

The auditory thresholds of different groups were determined by ABR detection. The detailed of the ABR test were described in our previous study [22]. Briefly, the mice were deeply anesthetized and three subcutaneous electrodes were placed at the vertex of the skull, the tested ear, and the contralateral ear. Click and tone burst stimuli at frequencies of 8, 16, 24, 32 and 40 kHz were generated. The responses were recorded and determined by decreasing sound intensities from 90 dB in 10 dB steps, which narrowed to 5 dB steps near the threshold. The lowest sound intensity that could be recognized was determined to be the auditory threshold.

Immunofluorescence

For activated caspase-3 immunostaining, mice were anesthetized and sacrificed at P6 or P11. For counting of cochlear HCs and DCs, mice (n = 4 in each group) were sacrificed at P18. The cochleae were carefully dissected in 0.01 M PBS and then fixed in 4% paraformaldehyde. For flattened cochlear preparations, the samples were rinsed three times with PBS and decalcified with 10% disodium EDTA at 4℃ for two days. Each stretched cochlear preparation was carefully dissected and incubated in blocking solution at room temperature for 1 h, then incubated with polyclonal rabbit anti-myosin 7a antibody (1:500 dilution, 25-6790, Proteus Bio-Sciences, Ramona, CA, USA), polyclonal goat anti-Sox2 antibodies (1:100 dilution, sc-17320, Santa Cruz Biotechnology, Santa Cruz, CA, USA), monoclonal rabbit anti-α-tubulin antibody (1:200 dilution, ab179484, Abcam, Cambridge, UK), or polyclonal rabbit anti-Cx30 antibodies (1:200 dilution, 40-7400, Invitrogen, Carlsbad, CA, USA). After washing with PBST for three times, then the samples were incubated with secondary fluorescent antibodies (1:200 dilution, ANT032, Antgene, Wuhan, China) for 2h in the dark. Phalloidin (P5282, Sigma, St Louis, MO, USA) was used for fluorescent visualization of HC F-actin and nuclei were labeled with DAPI (C1005, Beyotime Biotechnology, Jiangsu, China). All images were scanned with laser scanning confocal microscope (Nikon, Tokyo, Japan).

Resin sections and transmission electron microscopy (TEM)

The detailed methods for the TEM were given previously[23]. Briefly, mice were anesthetized and sacrificed at P18. After decalcification with 10% disodium EDTA for 48 h, each sample was then immersed in 1% osmium tetroxide to post-fix for 1 h. Samples were dehydrated through a graded ethanol series, before embedding in resin. Sections (1.5 μm in thickness) were stained with toluidine blue (89640-5G, Sigma-Aldrich) for observation, and ultrathin sections were stained with uranyl acetate and lead citrate and examined by TEM.

Scanning electron microscopy (SEM)

The morphology of HC stereocilia was observed by SEM at P18. As previously described[22], after fixation and decalcification, carefully dissected the cochleae to expose the basilar membrane. Then the samples were dehydrated in increasing ethanol concentrations, dried (HCP-2, Critical Point Dryer, HITACHI, Tokyo, Japan), and sputter-coated with a layer of gold (Eiko Engineering, Tokyo, Japan). Stereocilia bundles were observed in the three turns of the cochlea. Images were captured using a scanning electron microscope (VEGA 3 LMU, Tescan, Brno, Czech Republic).

FM1-43 Imaging

FM1-43 loading of HCs was used to assess the function of mechano-transduction channels. Mice (n = 4 in each group) were sacrificed at P18 and cochleae were quickly dissected from the temporal bones. The samples were incubated in a culture loaded with 4 μM FM1-43 (T35356, Invitrogen) for 30 s, and then fixed in 4% paraformaldehyde for 1 h. Samples were washed with 0.01 M PBS three times prior to imaging with a confocal microscope; all operations are performed at room temperature. DAPI was used for nuclear staining.

Real-time quantitative polymerase chain reaction (RT-qPCR)

Neonatal mice were injected with T3 at P0 for two successive days and then sacrificed at P4. The cochleae were removed and dissected in cold Hanks' balanced salt solution. The membranous cochlear duct sourced from one cochlea was used to generate one sample. The detailed methods for the RNA extraction and reverse transcribed were as described previously[24]. The RT-qPCR was performed in a Roche LightCycler 480 instrument (Roche Diagnostics Ltd, Switzerland). The transcriptional expression was normalized to the expression of GAPDH, and calculated the relative expression level between control and T3 group using the $2^{-\Delta\Delta CT}$ method.

Statistical analysis

Data are presented as means ± SEM and plotted using GraphPad Prism (Version 8.2.1, GraphPad Software Inc., La Jolla, CA, USA). Two-tailed, unpaired Student's t tests and two-way ANOVA were performed using SPSS software (Version 19, IBM SPSS Statistics, IBM Corp., Armonk, NY, USA), a value of $P < 0.05$ was considered to be statistically significant.

Results

Excessive T3 in the early postnatal days can induce hearing loss in mice

To evaluate the effect of T3 treatments at different postnatal periods on auditory function in mice, ABR was performed at P18. Compared with the control group, the ABR-click thresholds increased significantly in P0 or P1 group, while T3 given at P3 (P3 group) had no significant effects on ABR thresholds (Fig. 1A). Mice in P0 group showed severe deafness with mean thresholds above 80 dB SPL at 8–40 kHz, while mice in P1 group displayed moderate to severe deafness with hearing thresholds at 8, 16, 24, 32 and 40 kHz of 61.3 ± 6.3, 51.3 ± 2.5, 57.5 ± 9.6, 73.8 ± 7.5, 90.0 ± 0dB SPL, respectively (Fig. 1B). Mice treated with T3 at P3 showed normal hearing at P18 (Fig. 1B).

Excessive T3 accelerate the maturation of the greater epithelial ridge (GER) and do not affect hair cell survival

HC loss is a major cause of hearing loss. Thus, we analyzed the survival patterns of HCs in T3-treated mice. No substantial HC loss was observed in different T3 treated group at P18 (Fig. 2A–L). Although scattered losses of outer HCs were occasionally observed in the basal turn of P0 group (white arrows, Fig. 2F), statistical analysis showed that the number of OHCs was not significantly changed compared to the control group (n = 4, $P > 0.05$) (Fig. 2M).

In neonatal mice, the cochlea proceeded to develop structurally and functionally before hearing onset, and regression of the GER is a prominent structural changing event. During natural development, cells in GER promote the development and maturation of sensory epithelium through programmed cell death. We performed activated casapase-3 staining to determine the apoptosis pattern of GER in T3-treated mice. At P6, no activated caspase-3-positive (caspase-3+) cells were detected in the GER of control mice, while a large number of caspase-3+ cells were captured in GER of the T3-treated group (Fig. 2O–R). In contrast, caspase-3+ cells were evident in the GER of control cochleae and were not detected in the T3-treated group at P11 (Fig. 2S–V). Statistical analysis showed that the number of caspase-3+ cells differed significantly between the two groups at P6 and P11 (n = 4, $P < 0.01$) (Fig. 2N).

Excessive T3 interferes with the morphology of HC's stereocilia and function of MET channel

In mammals, stereocilia are located in the cuticular plate of the cochlear sensory cells and are responsible for converting mechanical vibrations generated by sound stimulation into electrical signals. Structural or functional defects of the stereocilia are one of the main causes of congenital or progressive deafness. We performed SEM to characterize the morphology of stereocilia in all turns of the cuticular plate in T3-treated mice. In the control group, three rows of stereocilia formed a V-shaped bundle in all three turns (Fig. 3A–C, a–c). However, treatment with T3 at P0 or P1 resulted in the stereocilia bundle of outer HCs in the apical and middle turns being disordered and losing their V-shaped structure, although

there were no obvious changes in morphology of the stereocilia bundle in the basal turn (Fig. 3D–I, d–i). In contrast the morphology and arrangement of the HC stereocilia bundle was almost unaffected when T3 was given at P3 (Fig. 3J–L, j–l). These results suggest that the abnormal arrangement of the HC stereocilia bundle may be strongly associated with hearing loss caused by excessive T3. In addition, FM1-43 loading of HCs was used to assess functional of MET channel. Compared with the control group, the uptake of FM1-43 by OHCs in the T3 treatment group was reduced (Fig. 3M–P). Quantitative results showed that the relative fluorescence density of FM1-43 in OHCs of T3-treated mice decreased by 23.9 ± 13.9% (Fig. 3Q). These results indicated that abnormalities of the HC stereocilia bundles and dysfunctions of MET channel might be responsible for the hearing loss induced by excessive T3.

Excessive T3 can induced overproduction of Deiter-like cells

To investigate the effect of T3 on remodeling of the OC in mice. Mice in P0 group were sacrificed at P18 and the SCs were labeled with Sox2. Furthermore, phalloidin was used to label the feet of the DCs and PCs. In the control group, the DCs were neatly arranged in three rows and the PCs were arranged in a single row in all turns (Fig. 4A–F). However, in P0 group, we observed four rows of DCs in the apical and middle turns, indicating the production of excess Deiter-like cells. In addition, the arrangement of Sox2-labeled SCs was disordered and the OPCs were jagged compared to the control group (Fig. 4G–J). The arrangement of DCs in the basal turn was almost unaffected in P0 group (Fig. 4K, L). Statistical analysis showed that the number of DCs was significantly increased in the apical and middle turns ($n = 4$, $P < 0.001$) (Fig. 4M). We also quantified the distance between inner pillar cells (IPCs) and OPCs and found that the relative distance between the feet of the IPCs and OPCs was reduced in the apical and middle turns P0 group, but there was no significant difference in the basal turn (Fig. 4N). Furthermore, we labeled DCs with Cx30, a protein subunit that constitutes gap junctions, which serves as a functional marker of DCs. In the control group, Cx30 signals (green) were evenly distributed along the boundaries of all DCs (Fig. 5B, D, F), whereas, in the T3 treatment group, we observed that the extra Deiter-like cells also expressed Cx30, which suggested that these cells might have partial functions of DCs (Fig. 5H, J, h, j). We quantified the number of Cx30+ DCs in all three turns of both groups, and found that the number of Cx30+ cells in the apical and middle turns of the T3 treatment group was significantly increased ($n = 4$, $P < 0.001$) (Fig. 5M).

Next, we explored the effects of excessive T3 administration at other time-points after birth on development of the OC in mice. When T3 was given at P1, we again observed the four rows of Cx30-expressing DCs in the apical and middle turns (Fig. 6D, d, E, e). However, T3 given at P3 did not significant effect the number of DCs (Fig. 6G–I, g–i). Quantitative results showed that the number of DCs was significantly increased in apical and middle turns from the P1 group ($n = 4$, $P < 0.001$) (Fig. 6J). The distance between the feet of the IPCs and OPCs was also reduced in the apical and middle turns of the P1 group (Fig. 6K). These parameters did not change significantly in the P3 group. Our results reveal that excessiveT3 can regulate the development of OC, especially for DCs, in a narrow postnatal time window.

Ultrastructural changes of SCs in T3 treated mice

Axial sections of the cochlea revealed the nuclei of three rows of DCs in the control group (Fig. 7A, B). However, in the apical turn of the T3-treated group, we clearly observed nuclei of four rows of DCs (Fig. 7C, D). Acetylated α-tubulin was used to label DCs and PCs, and this a proper maker to measure the supporting capacity of DC and PC. Three-dimensional reconstructed images showed that more than three rows of phalangeal processes were observed emanating from the foot of DCs in the T3-treated group (Fig. 7E, F). In addition, ultrastructural examination showed the presence of three rows of DC cell bodies in the control group and bundles of microtubules and normal mitochondria in the DCs (Fig. 7G–I). In P0 group, we observed four rows of DC cell bodies (Fig. 7J). The phalangeal processes of the extra DCs (DC4) showed normal architecture of the bundles of microtubules and mitochondria (Fig. 7K, L), which indicated that the overproduced Deiter-like cell have the similar structure and function as normal DCs.

Characterization of gene expression changes in the cochleae of T3-treated mice by realtime qPCR

In order to investigate the mechanism of T3 involved in the remodeling of the OC, we performed qPCR to analyze the expression levels of a series of genes regulating the development of inner ear. The mRNA expression of Atoh1 and Sox2, two transcription factors that regulate HCs and SCs' development, was significantly up-regulated (Fig. 8A). However, the other important factors Pou4f3, Neurog1, and Gfi1 did not change significantly. In addition, we analyzed the Notch, Wnt, TGFβ and FGF signaling pathways as well as cell cycle signaling pathways and found that the transcription levels of Notch pathway-related genes, such as Notch1, Notch2, Notch2, Notch3, Jag1, Jag2, Hey1, Hey2, Hes1, Hes5 and Dll1 were significantly down-regulated (Fig. 8B). The expression of FGF and most TGFβ signaling pathway genes did not change significantly, while only Smad4, Bmpr1b and Ltbp1 were downregulated (Fig. 8C, D). In the Wnt pathway, the mRNA expression levels of Lgr5 and Wnt2b were significantly down-regulated and other related genes were not significantly changed (Fig. 8E). In addition, we found that the cell cycle-dependent kinases Cdk2 and Cdk4, and cell division cyclin Cdc25c, were down-regulated in cochleae of T3-treated mice (Fig. 8F). All these results suggest that T3 may lead to overproduction of DCs mainly through down-regulation of the Notch signaling pathway in early cochlear development.

Downregulation of the Notch signaling pathway did not aggravate the overproduction of DCs induced by T3

Based on the above PCR results, we speculated that the Notch signaling pathway might be responsible for the overproduction of DCs induced by T3. To verify whether T3 combined with DAPT, an inhibitor of the Notch pathway, to synergistically regulate the additional increase of DCs, we treated mice with T3 and DAPT in combination, and then evaluated the DCs in the different groups at P18 (Fig. 9A). In the control and DAPT alone treated groups, three rows of DCs were neatly arranged, and Cx30 was observed at the edge of all DCs (Fig. 9B–G, b–g), which suggested that DAPT treatment alone did not affect the number of DCs. In the T3 and T3 combined with DAPT (T3+DAPT) treatment groups, four rows of DCs were observed in the apical and middle turns (Fig. 9H, I, K, L). Quantitative results showed no significant

difference in the number of DCs between the groups treated with T3 or T3+DAPT (Fig. 9N). In addition, we measured the distance between the feet of the IPCs and OPCs and found that the distance did not significantly differ between the groups treated with T3 and with T3+DAPT (Fig. 9M). These results suggest that T3 combined with inhibition of Notch signaling did not aggravate the overproduction of DCs induced by T3.

Effects of excessive T3 combined with down-regulated Sox2 on the remodeling of organ of Corti

Recent studies have shown that Sox2-CreER mice exhibit Sox2 haploid deficiency due to one of the alleles being replaced by CreER[25]. Using this characteristic, $Sox2^{CreER/+}$ mice were injected with T3 to explore the effect of T3 combined with Sox2 downregulation on the development of SCs in the inner ear (Fig. 10A). In $Sox2^{CreER/+}$ mice, three rows of DCs were neatly arranged, and Cx30 was observed at the edge of all DCs, almost as in the control group (Fig. 10B–G, b–g). In the T3 and the $Sox2^{CreER/+}$ + T3 groups, four rows of DCs were observed in the apical and middle turns, and the quantified results showed no significant difference in the number of DCs between the T3 and the $Sox2^{CreER/+}$ + T3 groups (Fig. 10N). However, two rows of OPCs were observed in the apical and middle turns of the $Sox2^{CreER/+}$ + T3 group (Fig. 10K, k, L, l). Statistical analysis showed that the number of OPCs was significantly increased in the apical and middle turns of the $Sox2^{CreER/+}$ + T3 group (n = 4, $P < 0.01$) (Fig. 10O). These results suggest that T3 combined with Sox2 downregulation did not aggravate the overproduction of DCs induced by T3, but did induce overproduction of OPCs. In addition, additional OPCs appear to form new TC (Fig. S1F).

Discussion

T3 is an exogenous factor involved in the stereocilia formation of cochlear hair cell

Over recent decades, a series of studies have focused on the role of thyroid hormones in fetal tissue differentiation and development[26]. Fetal nervous system development is highly sensitive to thyroid hormones, and maternal thyroid hormone disorder can cause fetal central nervous system symptoms including hearing, speech impairments, and squint[27]. Thyroid hormone-mediated apoptosis plays an important role in mammalian neurodevelopment. Apart from promoting maturation of the GER of mouse cochlea, thyroid hormone modifies the maturation and survival of cone photoreceptors responsible for color vision[28]. In this study, our results indicated that excessive administration of T3 in early postnatal day (P0 or P1) cans induce severe hearing loss in mice (Fig. 1). However, we did not observe significant degeneration of HC, suggesting that excessive T3 does not interferes with the survival of cochlear HC (Fig. 2A–L). In addition, caspase-3+ cells were detected in the GER of P0 group at P6, while apoptosis of the GER in the control group was not triggered at this time. Premature degeneration of GER triggered by

T3 resulted in advance opening of tunnel of Corti. However, it remains unclear whether pre-maturation of the OC is directly related to hearing loss.

Stereocilia are mechanical sensors located in the cochlear sensory cells that convert sound stimuli into electrical signals, and normal auditory function depends on the organization and morphology of the stereocilia, thus it is thought to be critical for mammalian hearing and balance[29, 30]. Disorders of the stereocilia hair bundle structure are involved in various congenital or progressive hearing loss[31–33]. Our study observed that administration of excessive T3 in the early postnatal stage (P0 or P1) caused disturbance in the arrangement of the stereocilia of HC, while the stereocilia showed normal structure when T3 was given at P3 (Fig. 3A–L). From the picture, the length of disordered stereocilia is longer than that of control. It seems that excessive T3 accelerate the growth of stereocilia of OHC. In addition, we observed that the reduced function of MET channels located at the apical junction of hair cell stereocilia in P0 group (Fig. 3M–P). It indicated that the ability of mechanoelectrical transduction of OHC was significantly impaired. Combined with analysis of the audiological phenotype and pathological phenotype, it was suggested that the disturbance of HC stereocilia was the main cause of hearing loss caused in P0 and P1 group. Based on the above results, excessive T3 at the early stage after birth does not affect HC survival but does cause dysfunction of HCs with the abnormal development of stereocilia, which would be a new mechanism of thyroid hormone-induced hearing loss.

T3 can regulated the production of SCs during critical periods of cochlear development

Thyroid hormone receptor, deiodinase and thyroid hormone transporter are widely expressed in the cochlea[34, 35], which suggest that cochleae are the targets of thyroid hormone regulation of inner ear development. Forrest et al. reported that T3 regulates cochlear remodeling, which involves premature regression of the GER [20]. However, the effect of T3 on remodeling of the OC during early development has not been further explored. Here, we observed that treatment with T3 in the early development stage (P0 or P1) resulted in overproduction of DCs. Immunostaining results showed that these cells were connected with adjacent DCs by gap junction. The microtubule, labeled by acetylated α-tubulin, was found in the body and phalangeal processes of the cell. It indicated that these Deiter-like cells may be functioning normally and can display intercellular communication with surrounding cells. Further speculation, it may be used as the preserve of DCs which can support new regenerated OHCs. Previous studies mainly focused on regulating SCs proliferation by regulating proliferation-related genes. Our study showed that endocrine signals also contribute to the regulation of SCs' proliferation. In addition, T3 administration at P3 did not affect the number of DCs, suggesting that there was a narrow time window during which T3 regulated the proliferation of SCs.

In adult mammals, damage to sensory cells in the inner ear causes permanent hearing loss because degeneration of HCs is irreversible, whereas HCs can spontaneously regenerate from supporting cells (SCs) after injury in birds and fish[36]. Recent studies have shown that HCs can also be regenerated from SCs in newborn mice[37–39], but this spontaneous regenerative ability rapidly diminishes with age.

Current research suggests that there are two mechanisms for HC regeneration in mammals, one of which is the direct trans-differentiation of SCs into new HCs[21]. In addition, the SCs or progenitor cells of the inner ear proliferate and then differentiate into new HCs[40–42]. The common feature of both pathways is that the new HCs are derived from SCs, which suggest that SCs in the inner ear are the key factor necessary for HC regeneration. Therefore, increasing the number of SCs is an important step in achieving HC regeneration. Multiple signaling pathways (Wnt, Notch, FGF, IGF and Shh) have been found to be involved in the development and proliferation of SCs, and down-regulation of related genes lead to an increase in the number of SCs in the inner ear[43–45]. Our results reveal that endocrine signals regulate the proliferation of inner ear SCs during critical periods of cochlear development, providing a reference to coordinate the multi-factor regulation of SC proliferation and HC regeneration.

Recent studies have shown that multiple signaling pathways are involved in regulating the development of HCs and SCs, among which the Notch signaling pathway plays an important role in this process [46]. In the sensory epithelium of the inner ear, HCs express the Notch ligands Dll1, Dll3, Dll4, Jag1 and Jag2, while SCs express Notch downstream genes including Hes1, Hes5, Hey1, Hey2, and HeyL. Notch-mediated lateral inhibition maintains SCs in a quiescent state, and suppression of Notch signaling by drugs or genetic ablation of Notch effector genes leads to excessive formation of HCs or overproduction of SCs[47, 48]. In our study, real-time quantitative PCR results showed that the expression of genes related to the Notch signaling pathway was significantly down-regulated, which might be involved in the overproduction of SCs. Furthermore, a combination of Notch inhibitors did not promote T3-induced overproduction of SCs, suggesting that Notch signaling is involved in T3-induced DC overproduction but its role is limited.

The combination of T3 and Sox2 can regulates not only the number of SCs but also the structure of OC

The expression of transcription factor Sox2 was significantly down-regulated in T3 group. Base on the characteristic of $Sox2^{CreER/+}$ mice with Sox2 haploinsufficiency[25], we constructed a mouse model of T3 combined with down-regulation of Sox2 by giving T3 to $Sox2^{CreER/+}$ mice. The results showed that excessive T3 treatment combined with downregulation of Sox2 not only resulted in overproduction of DCs, but also led to large number of OPCs. The exciting thing is that this extra OPC obviously in a more mature state with plenty of microtubules. In addition, extra TCs, which is a milestone for mature OC, can be formed to provide structural support for whole OC. This phenomenon indicates that T3 combined local transcription factors (such as Sox2) may regulate and even induce the formation of complex spatial structure of OC. Our findings may provide a theoretical basis for global OC regeneration. The key signaling pathway mediating SCs' proliferation and remodeling of OC's fine structure induced by T3 still needs further study. The idea that endocrine signaling may combine with gene programming to regulate cochlear development and support cell proliferation is a novel proposal which will open up new aspects of study and potentially lead to development of new therapies.

Conclusion

In conclusion, our results suggest that (I) T3 is an exogenous factor involved in the stereocilia formation of HC; (II) T3 regulated the production of SCs during critical periods of cochlear development; (III) The combination of T3 and Sox2 can regulates not only the number of SCs but also the structure of OC. Our findings provide new evidence for the role of endocrine signaling in regulating the development of cochlear sensory epithelium in the neonatal mice.

Declarations

Acknowledgements

This work was supported by grants from The National Nature Science Foundation of China (Nos: 81771003 and 82071508).

Conflict of interest

The authors declare that they have no conflict of interest.

Author Contributions

All authors contributed to the study conception and design. YS and SC conceived and designed the experiments; XB, KX and SC performed the experiments; KX and XB analyzed the data; KX, LX and YQ contributed the mouse breeding; XB and SC wrote the paper. YS reviewed and edited the manuscript. All authors read and approved the final manuscript.

Data Availability

The datasets generated are available from the corresponding author on reasonable request.

Ethics approval

All animal study was reviewed and approved by the Union Hospital of Tongji Medical College, Huazhong University of Science and Technology.

Consent to publish

All authors consent the publication of the manuscript in CMLS.

References

1. Wu DK, Kelley MW (2012) Molecular mechanisms of inner ear development. Cold Spring Harb Perspect Biol 4(8):a008409. doi:10.1101/cshperspect.a008409

2. Melnick M, Jaskoll T (2015) CMV-induced embryonic mouse organ of corti dysplasia: Network architecture of dysfunctional lateral inhibition. Birth defects research Part A, Clinical and molecular teratology. 103:573–582. 10.1002/bdra.23386. 7
3. Chen S, Xie L, Xu K, Cao HY, Wu X, Xu XX, Sun Y, Kong WJ (2018) Developmental abnormalities in supporting cell phalangeal processes and cytoskeleton in the Gjb2 knockdown mouse model. Dis Model Mech 11(2). doi:10.1242/dmm.033019
4. Uziel A, Marot M, Rabie A (1985) Corrective effects of thyroxine on cochlear abnormalities induced by congenital hypothyroidism in the rat. II. Electrophysiological study. Brain Res 351(1):123–127. doi:10.1016/0165-3806(85)90237-8
5. Driver EC, Kelley MW (2020) Development of the cochlea. Development 147(12). doi:10.1242/dev.162263
6. Groves AK, Fekete DM (2012) Shaping sound in space: the regulation of inner ear patterning. Development 139(2):245–257. doi:10.1242/dev.067074
7. Uziel A, Gabrion J, Ohresser M, Legrand C (1981) Effects of hypothyroidism on the structural development of the organ of Corti in the rat. Acta Otolaryngol 92(5–6):469–480. doi:10.3109/00016488109133286
8. Knipper M, Zinn C, Maier H, Praetorius M, Rohbock K, Köpschall I, Zimmermann U (2000) Thyroid hormone deficiency before the onset of hearing causes irreversible damage to peripheral and central auditory systems. J Neurophysiol 83(5):3101–3112. doi:10.1152/jn.2000.83.5.3101
9. Bianco AC, Salvatore D, Gereben B, Berry MJ, Larsen PR (2002) Biochemistry, cellular and molecular biology, and physiological roles of the iodothyronine selenodeiodinases. Endocr Rev 23(1):38–89. doi:10.1210/edrv.23.1.0455
10. St Germain DL, Galton VA, Hernandez A (2009) Minireview: Defining the roles of the iodothyronine deiodinases: current concepts and challenges. Endocrinology 150(3):1097–1107. doi:10.1210/en.2008-1588
11. DeLong GR, Stanbury JB, Fierro-Benitez R (1985) Neurological signs in congenital iodine-deficiency disorder (endemic cretinism). Dev Med Child Neurol 27(3):317–324. doi:10.1111/j.1469-8749.1985.tb04542.x
12. Lichtenberger-Geslin L, Dos Santos S, Hassani Y, Ecosse E, Van Den Abbeele T, Léger J (2013) Factors associated with hearing impairment in patients with congenital hypothyroidism treated since the neonatal period: a national population-based study. J Clin Endocrinol Metab 98(9):3644–3652. doi:10.1210/jc.2013-1645
13. Ferrara AM, Onigata K, Ercan O, Woodhead H, Weiss RE, Refetoff S (2012) Homozygous thyroid hormone receptor β-gene mutations in resistance to thyroid hormone: three new cases and review of the literature. J Clin Endocrinol Metab 97(4):1328–1336. doi:10.1210/jc.2011-2642
14. Griffith AJ, Szymko YM, Kaneshige M, Quiñónez RE, Kaneshige K, Heintz KA, Mastroianni MA, Kelley MW, Cheng SY (2002) Knock-in mouse model for resistance to thyroid hormone (RTH): an RTH

mutation in the thyroid hormone receptor beta gene disrupts cochlear morphogenesis. Journal of the Association for Research in Otolaryngology: JARO 3(3):279–288. doi:10.1007/s101620010092

15. Ng L, Kelley MW, Forrest D (2013) Making sense with thyroid hormone–the role of T(3) in auditory development. Nat Rev Endocrinol 9(5):296–307. doi:10.1038/nrendo.2013.58
16. Ng L, Goodyear RJ, Woods CA, Schneider MJ, Diamond E, Richardson GP, Kelley MW, Germain DL, Galton VA, Forrest D (2004) Hearing loss and retarded cochlear development in mice lacking type 2 iodothyronine deiodinase. Proc Natl Acad Sci U S A 101(10):3474–3479. doi:10.1073/pnas.0307402101
17. Rusch A, Ng L, Goodyear R, Oliver D, Lisoukov I, Vennstrom B, Richardson G, Kelley MW, Forrest D (2001) Retardation of cochlear maturation and impaired hair cell function caused by deletion of all known thyroid hormone receptors. The Journal of neuroscience: the official journal of the Society for Neuroscience 21(24):9792–9800. doi:10.1523/jneurosci.21-24-09792.2001
18. Mustapha M, Fang Q, Gong TW, Dolan DF, Raphael Y, Camper SA, Duncan RK (2009) Deafness and permanently reduced potassium channel gene expression and function in hypothyroid Pit1dw mutants. The Journal of neuroscience: the official journal of the Society for Neuroscience 29(4):1212–1223. doi:10.1523/jneurosci.4957-08.2009
19. Richter CP, Münscher A, Machado DS, Wondisford FE, Ortiga-Carvalho TM (2011) Complete activation of thyroid hormone receptor β by T3 is essential for normal cochlear function and morphology in mice. Cellular physiology and biochemistry: international journal of experimental cellular physiology biochemistry and pharmacology 28(5):997–1008. doi:10.1159/000335812
20. Peeters RP, Ng L, Ma M, Forrest D (2015) The timecourse of apoptotic cell death during postnatal remodeling of the mouse cochlea and its premature onset by triiodothyronine (T3). Mol Cell Endocrinol 407:1–8. doi:10.1016/j.mce.2015.02.025
21. Zhang S, Zhang Y, Dong Y, Guo L, Zhang Z, Shao B, Qi J, Zhou H, Zhu W, Yan X, Hong G, Zhang L, Zhang X, Tang M, Zhao C, Gao X, Chai R (2020) Knockdown of Foxg1 in supporting cells increases the trans-differentiation of supporting cells into hair cells in the neonatal mouse cochlea. Cell Mol Life Sci 77(7):1401–1419. doi:10.1007/s00018-019-03291-2
22. Chen S, Xu K, Xie L, Cao HY, Wu X, Du AN, He ZH, Lin X, Sun Y, Kong WJ (2018) The spatial distribution pattern of Connexin26 expression in supporting cells and its role in outer hair cell survival. Cell Death Dis 9(12):1180. doi:10.1038/s41419-018-1238-x
23. Xie L, Chen S, Xu K, Cao HY, Du AN, Bai X, Sun Y, Kong WJ (2019) Reduced postnatal expression of cochlear Connexin26 induces hearing loss and affects the developmental status of pillar cells in a dose-dependent manner. Neurochem Int 128:196–205. doi:10.1016/j.neuint.2019.04.012
24. Xu K, Chen S, Xie L, Qiu Y, Bai X, Liu XZ, Zhang HM, Wang XH, Jin Y, Sun Y, Kong WJ (2020) Local Macrophage-Related Immune Response Is Involved in Cochlear Epithelial Damage in Distinct Gjb2-Related Hereditary Deafness Models. Frontiers in cell and developmental biology 8:597769. doi:10.3389/fcell.2020.597769

25. Atkinson PJ, Dong Y, Gu S, Liu W, Najarro EH, Udagawa T, Cheng AG (2018) Sox2 haploinsufficiency primes regeneration and Wnt responsiveness in the mouse cochlea. J Clin Investig 128(4):1641–1656. doi:10.1172/jci97248
26. Prezioso G, Giannini C, Chiarelli F (2018) Effect of Thyroid Hormones on Neurons and Neurodevelopment. Hormone research in paediatrics 90(2):73–81. doi:10.1159/000492129
27. Moog NK, Entringer S, Heim C, Wadhwa PD, Kathmann N, Buss C (2017) Influence of maternal thyroid hormones during gestation on fetal brain development. Neuroscience 342:68–100. doi:10.1016/j.neuroscience.2015.09.070
28. Ng L, Lyubarsky A, Nikonov SS, Ma M, Srinivas M, Kefas B, St Germain DL, Hernandez A, Pugh EN Jr, Forrest D (2010) Type 3 deiodinase, a thyroid-hormone-inactivating enzyme, controls survival and maturation of cone photoreceptors. The Journal of neuroscience: the official journal of the Society for Neuroscience 30(9):3347–3357. doi:10.1523/jneurosci.5267-09.2010
29. Gillespie PG, Müller U (2009) Mechanotransduction by hair cells: models, molecules, and mechanisms. Cell 139(1):33–44. doi:10.1016/j.cell.2009.09.010
30. Hudspeth AJ (2008) Making an effort to listen: mechanical amplification in the ear. Neuron 59(4):530–545. doi:10.1016/j.neuron.2008.07.012
31. Liu Y, Qi J, Chen X, Tang M, Chu C, Zhu W, Li H, Tian C, Yang G, Zhong C, Zhang Y, Ni G, He S, Chai R, Zhong G (2019) Critical role of spectrin in hearing development and deafness. Sci Adv 5(4):eaav7803. doi:10.1126/sciadv.aav7803
32. Katsuno T, Belyantseva IA, Cartagena-Rivera AX, Ohta K, Crump SM, Petralia RS, Ono K, Tona R, Imtiaz A, Rehman A, Kiyonari H, Kaneko M, Wang YX, Abe T, Ikeya M, Fenollar-Ferrer C, Riordan GP, Wilson EA, Fitzgerald TS, Segawa K, Omori K, Ito J, Frolenkov GI, Friedman TB, Kitajiri SI (2019) TRIOBP-5 sculpts stereocilia rootlets and stiffens supporting cells enabling hearing. JCI insight 4(12). doi:10.1172/jci.insight.128561
33. Liu C, Luo N, Tung CY, Perrin BJ, Zhao B (2018) GRXCR2 Regulates Taperin Localization Critical for Stereocilia Morphology and Hearing. Cell reports 25(5):1268–1280e1264. doi:10.1016/j.celrep.2018.09.063
34. Ng L, Hernandez A, He W, Ren T, Srinivas M, Ma M, Galton VA, St Germain DL, Forrest D (2009) A protective role for type 3 deiodinase, a thyroid hormone-inactivating enzyme, in cochlear development and auditory function. Endocrinology 150(4):1952–1960. doi:10.1210/en.2008-1419
35. Sharlin DS, Visser TJ, Forrest D (2011) Developmental and cell-specific expression of thyroid hormone transporters in the mouse cochlea. Endocrinology 152(12):5053–5064. doi:10.1210/en.2011-1372
36. Rubel EW, Furrer SA, Stone JS (2013) A brief history of hair cell regeneration research and speculations on the future. Hear Res 297:42–51. doi:10.1016/j.heares.2012.12.014
37. Bramhall NF, Shi F, Arnold K, Hochedlinger K, Edge AS (2014) Lgr5-positive supporting cells generate new hair cells in the postnatal cochlea. Stem cell reports 2(3):311–322. doi:10.1016/j.stemcr.2014.01.008

38. Chai R, Kuo B, Wang T, Liaw EJ, Xia A, Jan TA, Liu Z, Taketo MM, Oghalai JS, Nusse R, Zuo J, Cheng AG (2012) Wnt signaling induces proliferation of sensory precursors in the postnatal mouse cochlea. Proc Natl Acad Sci U S A 109(21):8167–8172. doi:10.1073/pnas.1202774109
39. Zhang Y, Guo L, Lu X, Cheng C, Sun S, Li W, Zhao L, Lai C, Zhang S, Yu C, Tang M, Chen Y, Chai R, Li H (2018) Characterization of Lgr6+ Cells as an Enriched Population of Hair Cell Progenitors Compared to Lgr5+ Cells for Hair Cell Generation in the Neonatal Mouse Cochlea. Front Mol Neurosci 11:147. doi:10.3389/fnmol.2018.00147
40. Shi F, Kempfle JS, Edge AS (2012) Wnt-responsive Lgr5-expressing stem cells are hair cell progenitors in the cochlea. The Journal of neuroscience: the official journal of the Society for Neuroscience 32(28):9639–9648. doi:10.1523/jneurosci.1064-12.2012
41. Lush ME, Diaz DC, Koenecke N, Baek S, Boldt H, St Peter MK, Gaitan-Escudero T, Romero-Carvajal A, Busch-Nentwich EM, Perera AG, Hall KE, Peak A, Haug JS, Piotrowski T (2019) scRNA-Seq reveals distinct stem cell populations that drive hair cell regeneration after loss of Fgf and Notch signaling. eLife 8. doi:10.7554/eLife.44431
42. Cox BC, Chai R, Lenoir A, Liu Z, Zhang L, Nguyen DH, Chalasani K, Steigelman KA, Fang J, Rubel EW, Cheng AG, Zuo J (2014) Spontaneous hair cell regeneration in the neonatal mouse cochlea in vivo. Development 141(4):816–829. doi:10.1242/dev.103036
43. Rocha-Sanchez SM, Scheetz LR, Contreras M, Weston MD, Korte M, McGee J, Walsh EJ (2011) Mature mice lacking Rbl2/p130 gene have supernumerary inner ear hair cells and supporting cells. The Journal of neuroscience: the official journal of the Society for Neuroscience 31(24):8883–8893. doi:10.1523/jneurosci.5821-10.2011
44. Tateya T, Imayoshi I, Tateya I, Ito J, Kageyama R (2011) Cooperative functions of Hes/Hey genes in auditory hair cell and supporting cell development. Dev Biol 352(2):329–340. doi:10.1016/j.ydbio.2011.01.038
45. Maass JC, Berndt FA, Cánovas J, Kukuljan M (2013) p27Kip1 knockdown induces proliferation in the organ of Corti in culture after efficient shRNA lentiviral transduction. Journal of the Association for Research in Otolaryngology: JARO 14(4):495–508. doi:10.1007/s10162-013-0383-2
46. Kelley MW (2006) Regulation of cell fate in the sensory epithelia of the inner ear. Nat Rev Neurosci 7(11):837–849. doi:10.1038/nrn1987
47. Kiernan AE, Cordes R, Kopan R, Gossler A, Gridley T (2005) The Notch ligands DLL1 and JAG2 act synergistically to regulate hair cell development in the mammalian inner ear. Development 132(19):4353–4362. doi:10.1242/dev.02002
48. Li S, Mark S, Radde-Gallwitz K, Schlisner R, Chin MT, Chen P (2008) Hey2 functions in parallel with Hes1 and Hes5 for mammalian auditory sensory organ development. BMC Dev Biol 8:20. doi:10.1186/1471-213x-8-20

Figures

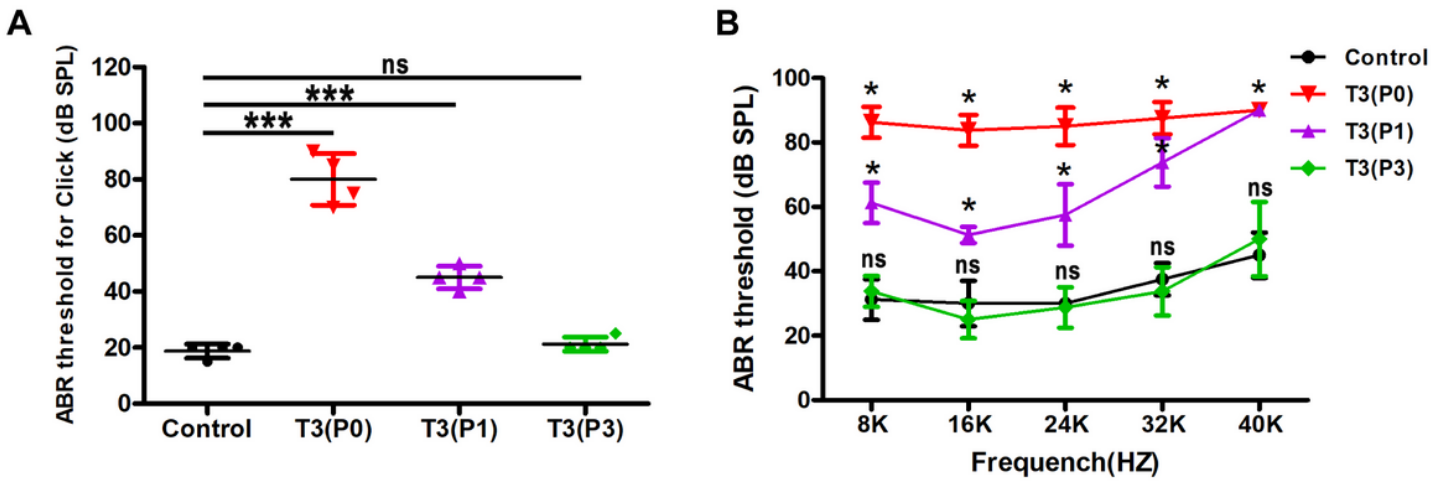

Figure 1

Excessive T3 in the early postnatal days can induce hearing loss in mice. (A) ABR-click thresholds in control and different treatment groups. (B) Comparison of tone-burst thresholds in different groups. ns: not significant, *P < 0.05, *** P < 0.001.

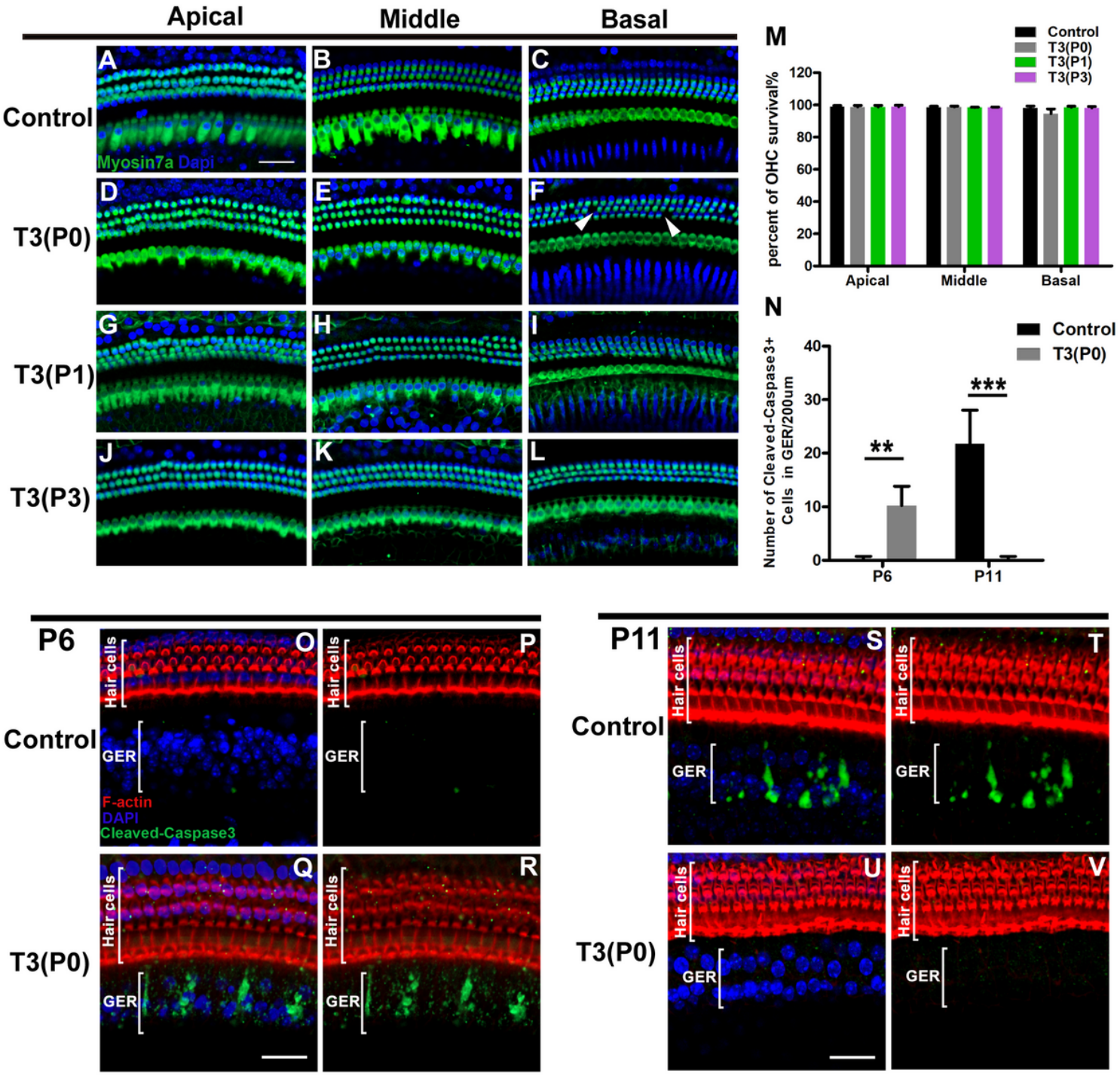

Figure 2

Excessive T3 accelerate the maturation of GER. (A-L) Representative confocal images of HCs (Myosin7a, green) of apical, middle and basal turns in different group at P18. White arrows indicate the sporadic missing OHCs (F). (M) Quantifications of OHCs survival in three turns of different groups at P18. (O, P) Representative images of caspase3^{+} cells in GER of apical turns in control group at P6. (Q, R) Representative images of caspase3^{+} cells in GER of apical turns in T3 treatment group at P6. (S-V) Representative images of caspase3^{+} cells in GER of apical turns in different group at P11. (N)

Quantifications of caspase3^{+} cells of GER in the apical turn of different groups at P6 and P11. *Significantly different from control group (** P<0.01, ***P <0.001). Scale bar: 40 μm (A, Q, U).

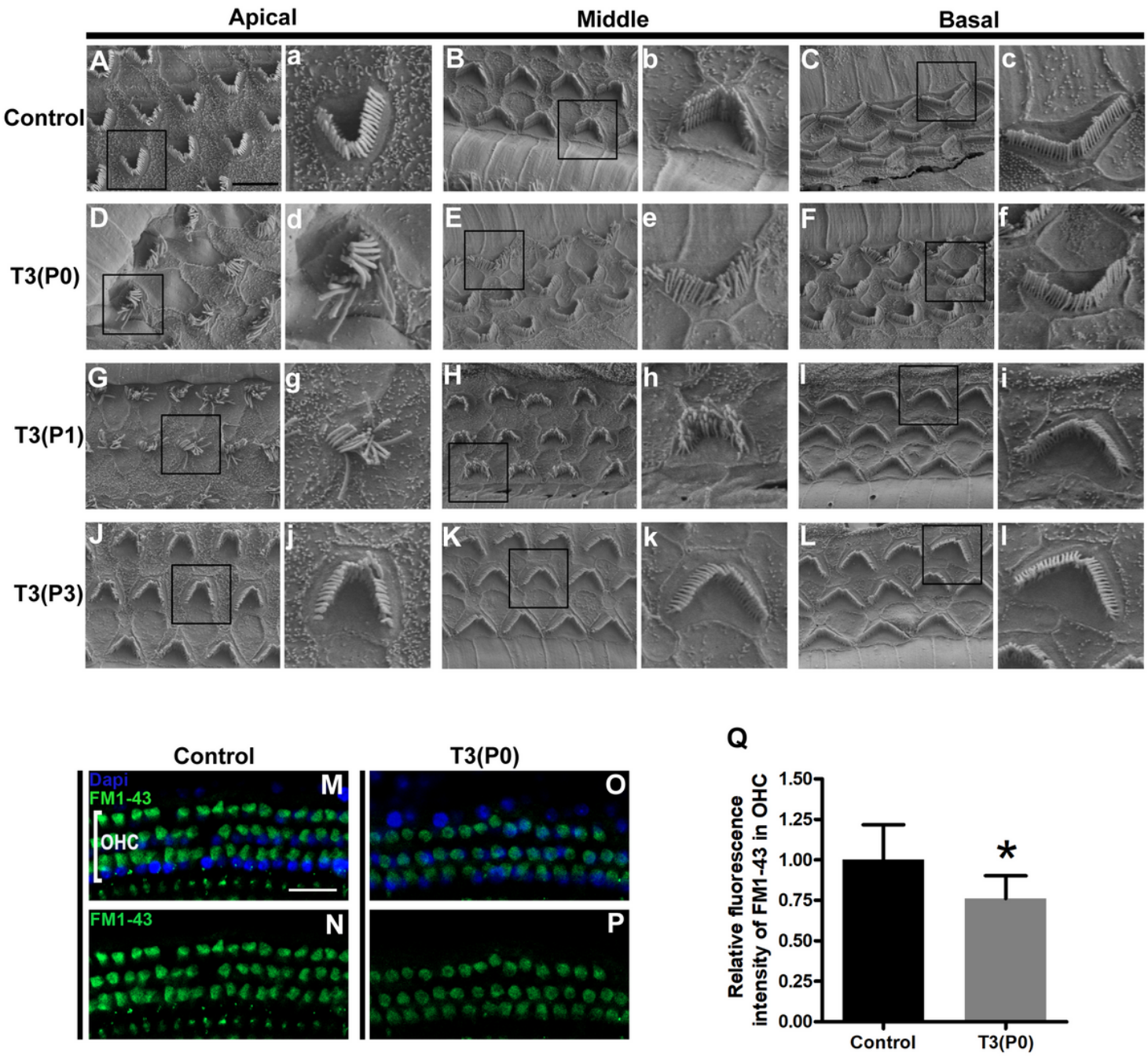

Figure 3

Excessive T3 interferes with the morphology of HC's stereocilia and function of MET channel (A-C) The morphology of the hair cells stereocilia in different turns of control group. (a-c) Magnifications of the stereocilia in different turns of control group. (D-L) Representative images of the hair cells stereocilia in

the apical, middle, and basal turns of different T3 treatment group. (d-l) Magnified images show the morphology of the stereocilia in different group. (M-P) Representative images of FM1-43 uptake by OHCs in the control and P0 T3 treatment group. (Q) Quantification of FM1-43 fluorescence in OHCs in different group. *Significantly different from control group (* P<0.05). The scales in panel A and M represent 10 and 40 μm, respectively.

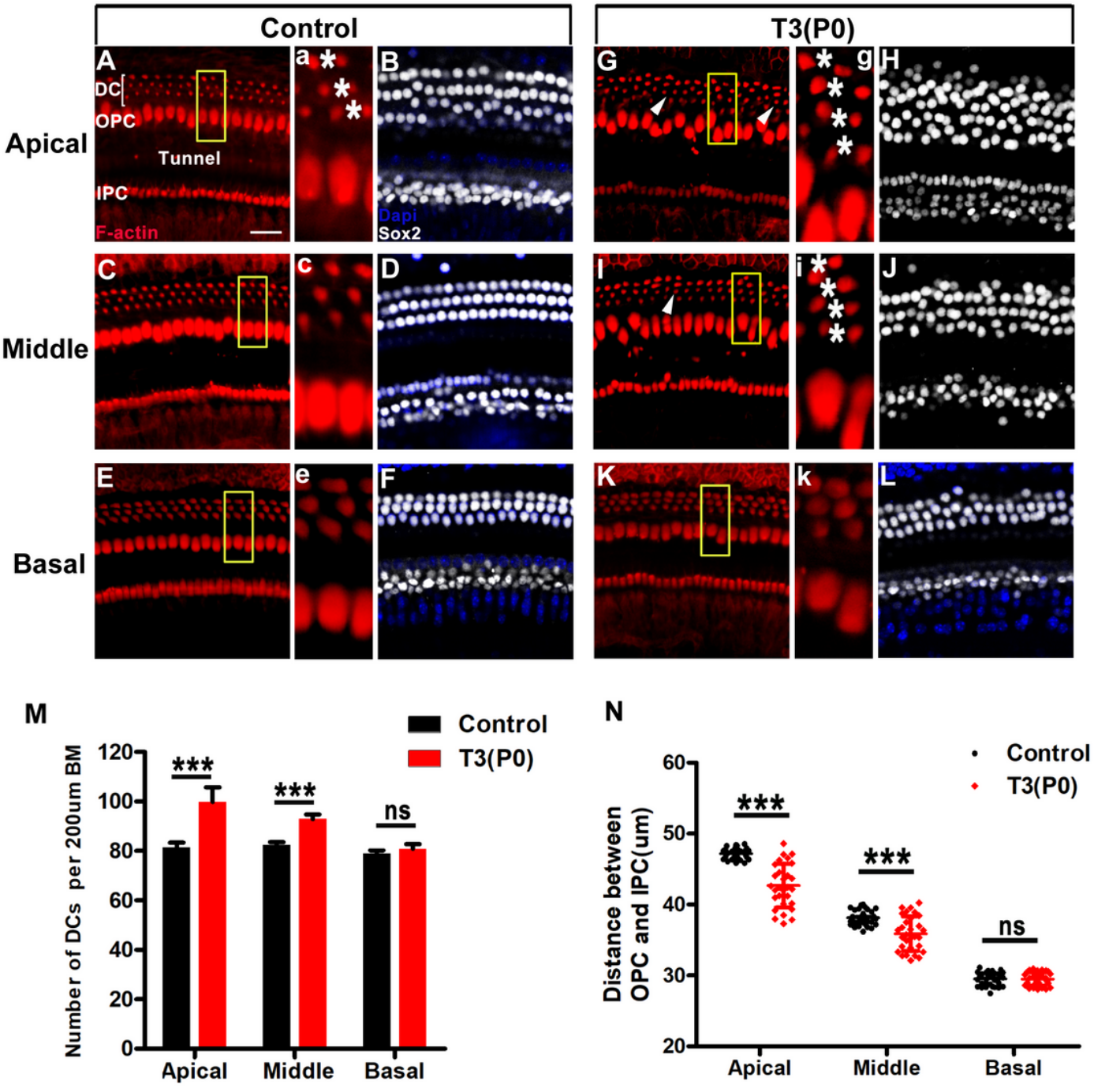

Figure 4

Excessive T3 can induced overproduction of DCs. (A, C, E) Representative images of DCs (F-actin, red) of different turns in control group at P18. (a, c, e) Magnified images of yellow boxes in panel A, C, E. (B, D, F) Representative images of SCs (Sox2, white) of different turns in control group at P18. (G, I, K) Representative images of DCs (F-actin, red) of apical, middle and basal turns in T3 treatment group at P18. White arrowheads indicate the extra DCs in the T3 treatment group (G and I). (g, i, k) Magnified images of yellow boxes in panel G, I, K. The asterisk indicates that DCs are arranged in four rows in apical and middle turn of T3 treatment group (g, i). (H, J, L) Representative images of SCs of different turns in T3 treatment group at P18. (M) Comparison of the number of DCs at specific cochlear locations in control and T3 treatment groups. (N) Comparison of the distance between the foot of IPCs and OPCs in the different groups. ns: not significant, *** P<0.001. Scale bar: 40 μm (A).

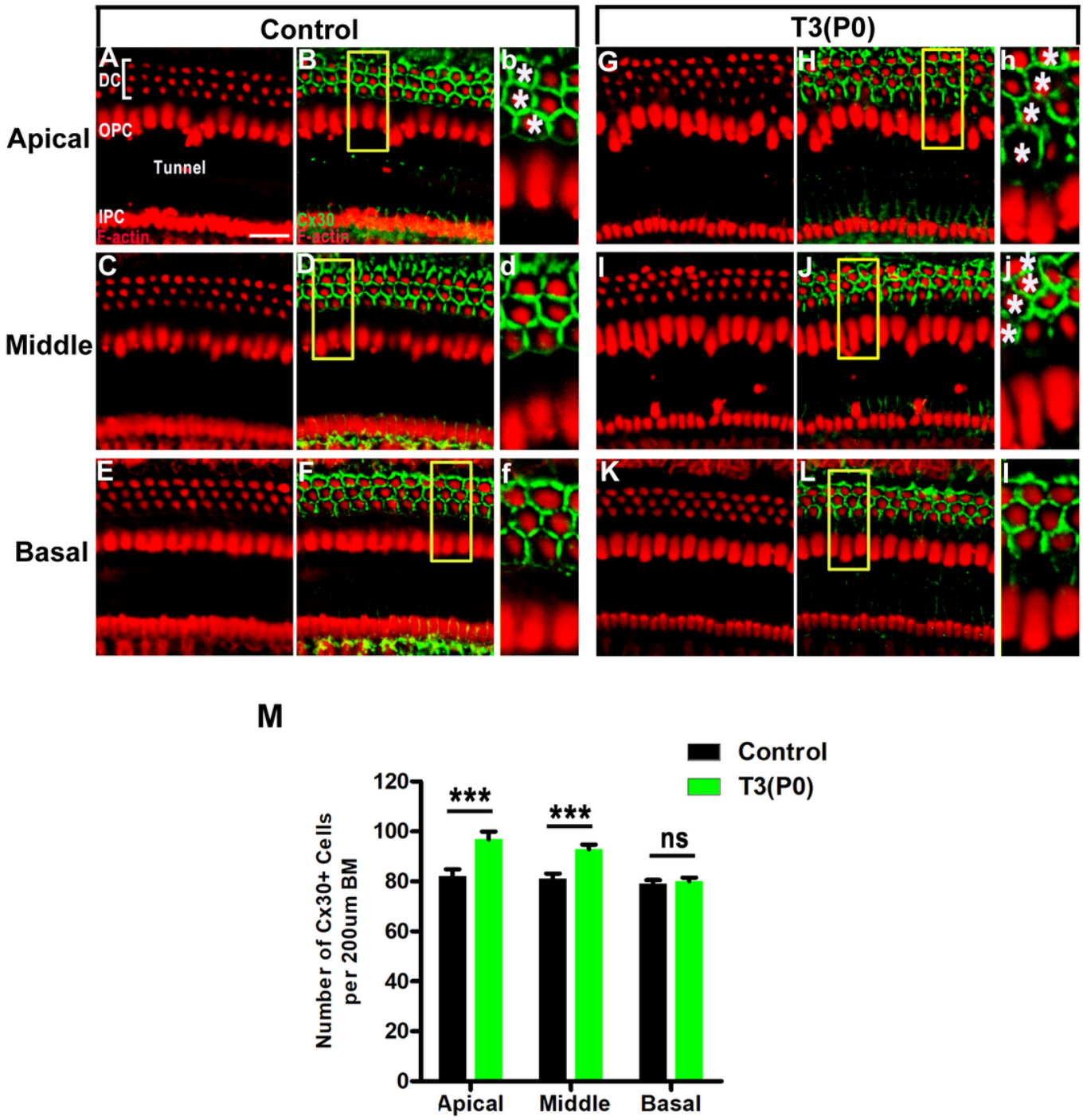

Figure 5

Extra DCs express gap junctions. (A-F) F-actin (red) and Cx30 immunolabeling (green) in different turns of the control group, respectively. (b, d, f) Magnified images of yellow boxes in panel B, D, F. Asterisk indicates DCs were arranged in three rows in control group (b). (G-L) F-actin and Cx30 immunolabeling in all three turns of the T3 treatment group, respectively. (h, j, l) Magnified images of yellow boxes in panel H, J, L. The asterisk indicates the region that DCs were arranged in four rows in the apical and middle

turns of T3 treatment group (h, j). (M) Quantifications of Cx30+ DCs number at specific cochlear locations in the different groups at P18. ns: not significant, *** P<0.001. Scale bar: 40 μm (A).

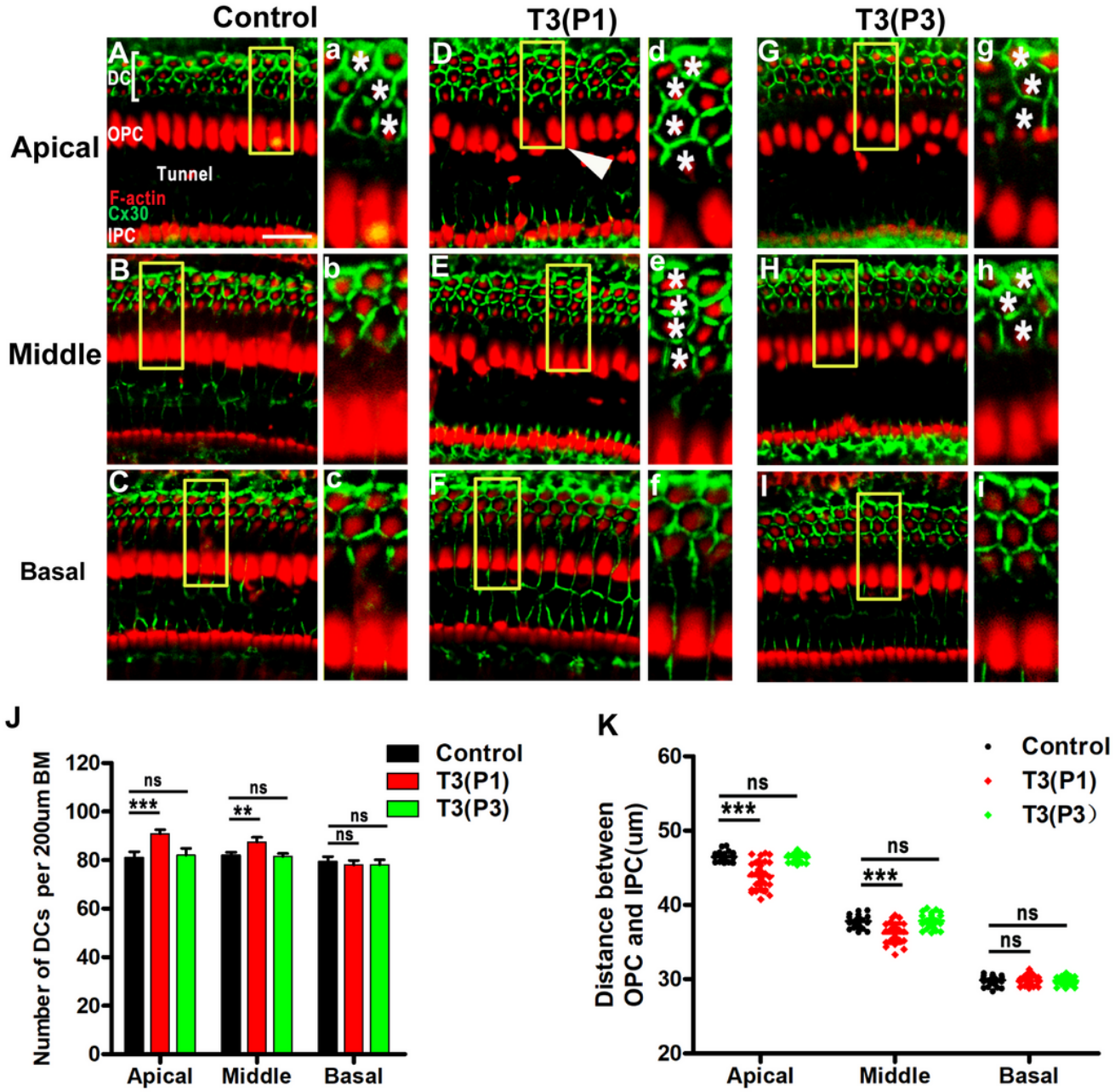

Figure 6

Extra DCs can be only induced by T3 in early postnatal day. (A-C) F-actin (red) and Cx30 immunolabeling (green) in all turns of the control group, respectively. (a-c) Magnified images of yellow boxes in panel A-C. Asterisk indicates DCs were arranged in three rows in control group (a). (D-F) Representative images of DCs and Cx30 expression patterns of different turns in T3 treated at P1(P1 T3) group, respectively. (d-f) Magnified images of yellow boxes in panel D-F. The asterisk indicates the region that DCs were arranged in four rows in the apical and middle turns (d, e), and White arrowheads indicate the arrangement of OPCs were jagged in the T3 treatment group. (G-I) Representative images of DCs and Cx30 expression

patterns of apical, middle and basal turns of T3 treated at P3(P3 T3) group, respectively. (g-i) Magnified images of yellow boxes in panel G-I. The asterisk indicates that the DCs were arranged in three rows (g, h), which similar to the control group. (J) Quantifications of the number of DCs at specific cochlear locations in the different groups at P18. (K) Comparison of the distance between the foot of IPCs and OPCs in the different groups. ns: not significant, ** P<0.01, *** P<0.001. Scale bar: 40 μm (A).

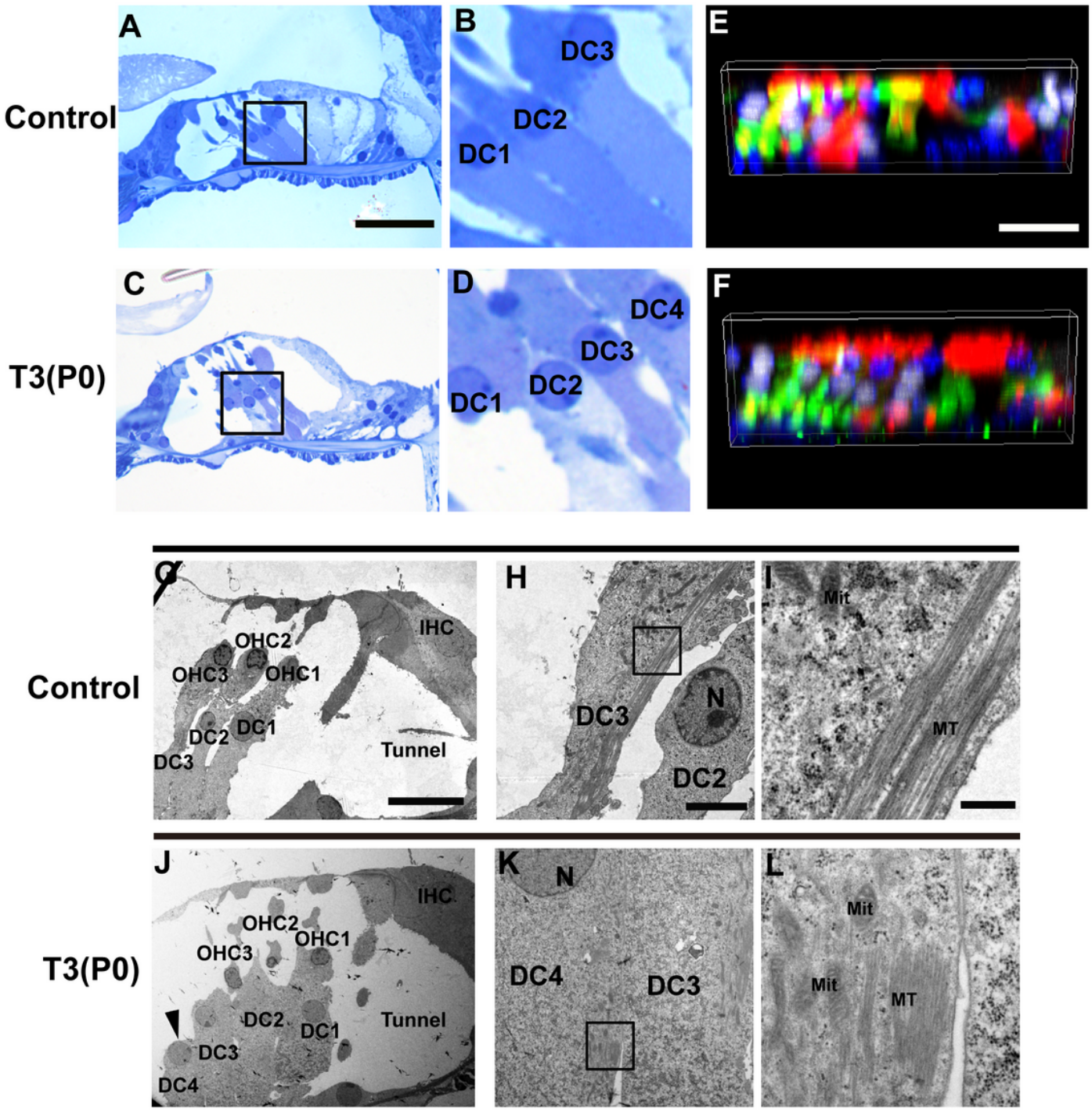

Figure 7

Ultrastructural observation of extra DCs (DC4) induced by T3. (A, C) The morphology of the OC in the apical of the control group and T3 treatment group at P18. (B, D) Magnified images of black boxes in panel A and C. (E, F). (G) The ultrastructure of OC in apical turns from control group. (H, I) Magnified images show the ultrastructural of DCs in control group. (J) The ultrastructure of OC in apical turns from the T3 treatment group. The black arrowhead in panel J indicates the extra DCs (DC4). (K, L) Magnified images show the ultrastructural of DC4 in the T3 treatment group. The scales in panel A, G, H and I represent 40, 20, 5 and 0.5 μm, respectively. N: nucleus, MT: microtubule, Mit: mitochondria.

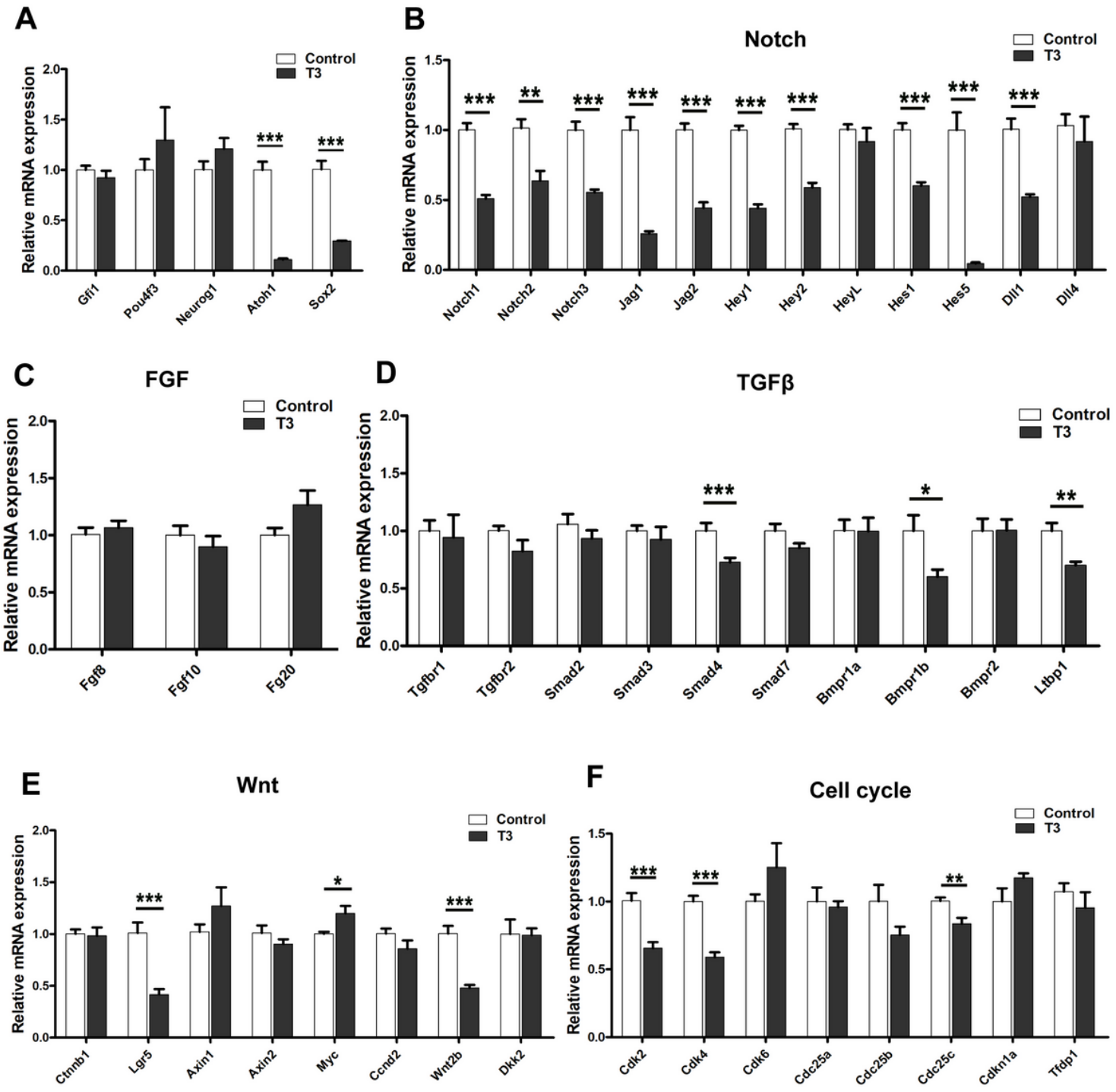

Figure 8

Characterization of gene expression changes in the cochlea of T3 treated mice. (A-F) Relative mRNA expression levels of genes related to SCs development (A), Notch signaling (B), FGF signaling (C), TGFβ signaling (D), Wnt signaling (E) and cell cycle pathways (F). *P <0.05, ** P<0.01, ***P <0.001.

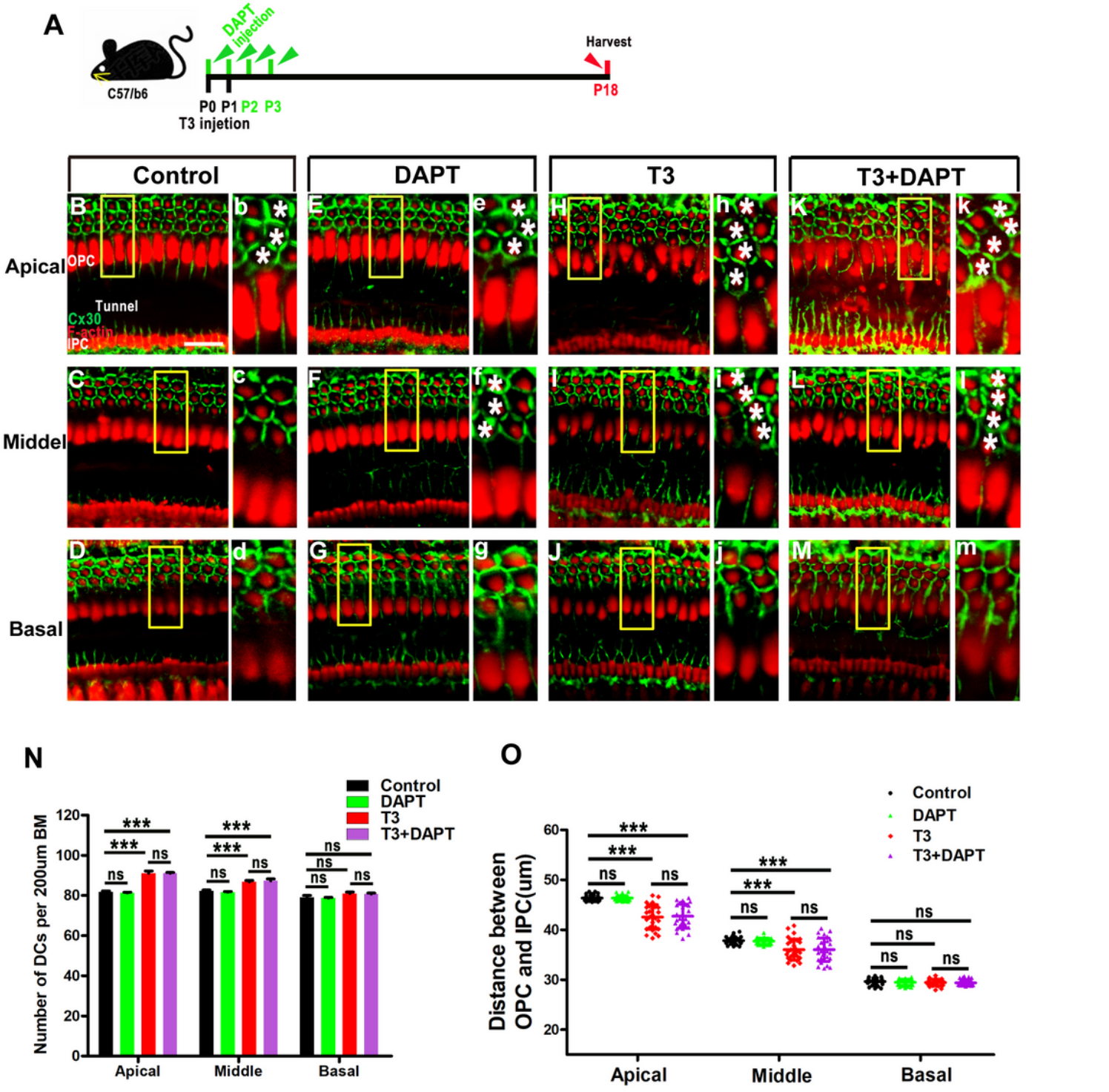

Figure 9

Effects of T3 combined with inhibition of Notch signaling pathway on DCs. (A) T3 was injected at P0 and P1, meanwhile, DAPT was injected at P0-P3 and was sacrificed at P18. (B-D) F-actin (red) and Cx30 immunolabeling (green) in different turns of the control group. (b-d) Magnified images of yellow boxes in panel B-D. (E-G) Representative images of DCs and Cx30 expression patterns of different turns of DAPT treated group, respectively. (e-g) Magnified images of yellow boxes in panel E-G. Asterisk indicates DCs were arranged in three rows in DAPT treatment group. (H-J) Representative images of DCs and Cx30 expression patterns of all three turns of T3 treatment group, respectively. Asterisk indicates DCs were arranged in four rows in apical and middle turns of T3 treatment group (h, i). (K-L) Representative images of DCs and Cx30 expression patterns in different turns of T3 combined with DAPT treatment group. Asterisk indicates DCs were arranged in four rows in apical and middle turns (k, l), which was similar to treated with T3 alone. (N) Comparison of the number of DCs at specific locations in the different groups. (O) Comparison of the distance between the foot of IPCs and OPCs in the different groups. ns: not significant, *** $P<0.001$. Scale bar: 40 μm (B).

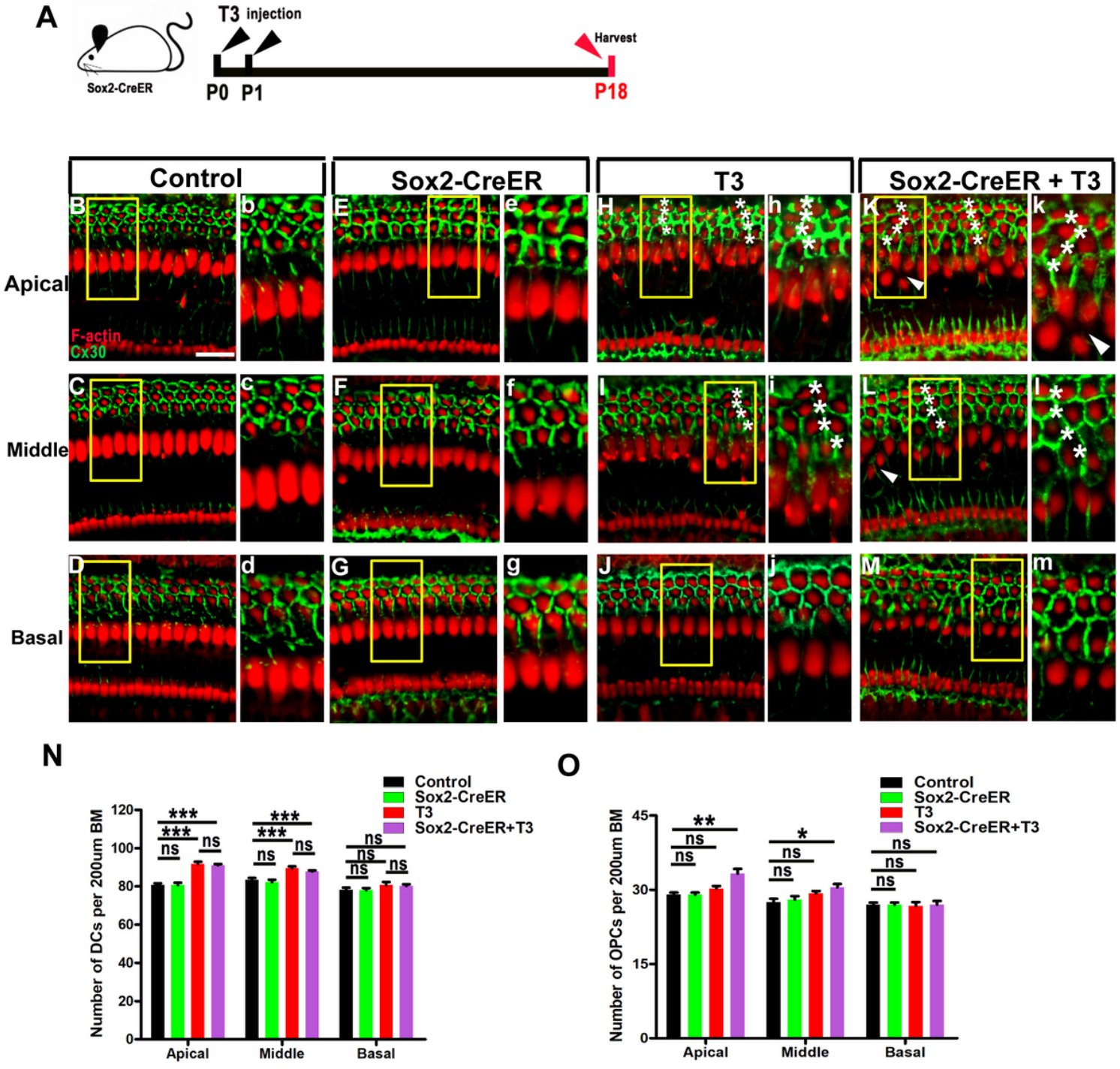

Figure 10

Effects of T3 combined with down regulating Sox2 on the remodeling of OC. (A) Sox2-CreER mice were injected with T3 at P0 and P1, and sacrificed at P18. (B-D) F-actin (red) and Cx30 immunolabeling (green) in different turns of the control group. (E-G) Representative images of DCs and Cx30 expression patterns of different turns of Sox2-CreER mice. (b-g) Magnified images of yellow boxes in panel B-G. (H-J) Representative images of DCs and Cx30 expression patterns of apical, middle and basal turns of alone treated with T3 group, respectively. Asterisk indicates DCs were arranged in four rows in apical and

middle turns of T3 alone treated group (H, I, h, i). (K-L) Representative images of DCs and Cx30 expression patterns in different turns of T3 combined with down regulating Sox2 group. Asterisk indicates DCs were arranged in four rows in apical and middle turns (K, L, k, l), and White arrowheads indicate the regions that OPCs were arranged in two rows in apical and middle turns (K, L). (N) Comparison of the number of DCs at specific cochlear locations in the different groups. (O) Comparison of the number of OPCs at specific cochlear locations in the different groups. ns: not significant, *** P<0.001, ** P<0.01, * P<0.05. Scale bar: 40 μm (B).

Supplementary Files

This is a list of supplementary files associated with this preprint. Click to download.

- FigureS1.tif